Sensors and Actuators A 299 (2019) 111630

Contents lists available at ScienceDirect

Sensors and Actuators A: Physical

journal homepage: www.elsevier.com/locate/sna

Tape'n roll inertial microfluidics

Mohammad Asghari [a], Murat Serhatlioglu [a], Resul Saritas [b], Mustafa Tahsin Guler [c], Caglar Elbuken [a,*]

[a] UNAM - National Nanotechnology Research Center, Institute of Materials Science and Nanotechnology, Bilkent University, 06800, Ankara, Turkey
[b] Department of Systems Design Engineering, University of Waterloo, Waterloo, ON, N2L 3G1, Canada
[c] Department of Physics, Kirikkale University, 71450, Kirikkale, Turkey

ARTICLE INFO

Article history:
Received 24 April 2019
Received in revised form 1 September 2019
Accepted 19 September 2019
Available online 20 September 2019

Keywords:
Particle focusing
Inertial focusing
3D microfluidics
Flexible microfluidics

ABSTRACT

Particle focusing and separation in microfluidic devices are critical for biological and medical applications. Inertial microfluidics is used for high throughput bio-particle focusing and separation. Most of the inertial microfluidic systems use planar structures for squeezing the particles in streams. Particle manipulation in 3D structures is often overlooked due to the complexity of the fabrication. In this study, we introduce some novel microchannel designs for inertial microfluidics by using a simple fabrication method that allows construction of both 2D and 3D structures. First, inertial migration of particles in 2D layouts including straight, spiral, and square spiral channels is investigated. Afterward, by applying a "tape'n roll" method, helical and double oriented spiral channels are configured and unexplored inertial migration behaviours are observed. Thanks to the simplicity of the fabrication and the unique characteristics of the new designs, high performance microfluidic inertial migration results can be obtained without any need for complicated microfabrication steps. The design optimization cycle can also be shortened using a computational approach we introduce in this study.

1. Introduction

Particle manipulation in micro scale is an important topic of research due to its applications in biomedical and clinical research [1–3]. Confinement and separation of particles based on their size can be achieved by exploiting the medium's rheological properties, optimizing channel geometry, or a combination of them. The use of external fields for particle manipulation such as electrical [4], optical [5], magnetic [6], and acoustic [7] fields has been extensively studied. More recently, passive particle manipulation approaches have gained traction relying on inertial [8] and viscoelastic [9] effects. Particle manipulation using inertial microfluidics depends mainly on flow conditions and channel geometry. For viscoelastic fluids, on the other hand, rheological properties of the fluid can generate elastic force and affect particle motion [10,11]. So far inertial focusing has been more commonly employed due to its simplicity and higher throughput. Inertial migration of particles has been demonstrated in channels with different structures and cross sections for various purposes including sheathless focusing for flow cytometry [12,13], steady inter-particle spacing for single cell analysis [14,15], cell trapping [16,17], size- [18–20], and shape-based [21,22] particle separation. Most of these studies investigated particle migration in planar structures using straight [23], spiral [19,24,25], and serpentine [23,26,27] microchannels. Curved microchannels, such as spiral and serpentine, create vortices in orthogonal direction of the flow direction thus introduce flexibility for particle manipulation by creating secondary forces. In spiral channels, magnitude of the Dean flow changes due to the continuous change in radius of curvature along the microchannel. The focusing mechanism in the serpentine microchannel is more complex due to the change in the direction in addition to the magnitude of the secondary flow. To keep both the direction and magnitude constant, one solution is to construct 3D helical structures with constant radius of curvature. Despite the voluminous literature on inertial focusing, a simple solution for 3D helical microstructures with optimal focusing performance has not been elucidated.

In this study, we analyse particle motion within inertial regime inside 2D and 3D structures. In order to produce 2D and 3D structures without cumbersome microfabrication methods, we present a surprisingly simple, yet effective, fabrication method that uses a microchannel fabricated by conventional soft lithography. The monolithic PDMS microchannel with rectangular cross section is sealed by polyimide tape (Kapton®). Spiral, straight, and square spiral (squarel) channels are sealed with tape and used in a 2D

* Corresponding author.
E-mail address: elbuken@unam.bilkent.edu.tr (C. Elbuken).

https://doi.org/10.1016/j.sna.2019.111630
0924-4247/

planar configuration. For 3D structures, after sealing the structure with the tape, the system is rolled around a rod to produce helical and double oriented spiral structures. The geometrical parameters of the structures (radius of curvature and pitch of helix) can easily be adjusted. This method offers great advantages compared to conventional fabrication techniques. It enables the transformation of planar layouts to 3D geometries. Additionally, planar layouts of different cross sections such as square [27], rectangular [28], triangular [29], semi-circular [30], and trapezoidal [19] shapes can be morphed into 3D channels. An additional benefit of this structure is that in case of channel clogging, the device can be reused by simply resealing the microchannel using new tape. An analysis of bonding strength for resealed devices is given in supplementary file. Finally, the flexibility of the system allows the fabricated structures to be used in a range of applications including wearable microdevices and healthcare systems [31]. Additionally, we introduce a computational method to study design optimization for 3D inertial focusing structures, which had mostly been studied experimentally thus far. Using this approach, it is possible to have better insight for particle motion along the channel. Our results show that particles travelling in a helical pathway inside a rectangular channel get focused in an elliptic profile across the channel cross section.

1.1. Inertial microfluidics theory

Inertial microfluidics study systems in micro scale where fluid's inertial effects are non-negligible and influence the movement of suspended particles across fluid streamlines. This phenomenon occurs at sufficiently high Reynolds numbers when inertial lift forces for a specific size of particle become dominant, and can transfer suspended particles between the fluid streamlines. Two dominant inertial lift forces are shear gradient lift force originating from parabolic flow velocity profile and wall lift force due to the asymmetric flow field around the particle in the presence of the boundaries. The net lift force is the sum of these inertial lift forces and exhibits the potential to be used for particle focusing and separation applications. The earliest study of inertial effect was investigated by Segre and Silberberg where they showed that rigid millimeter-size particles in a cylindrical pipe migrate to the equilibrium position of an annulus shape with radius of 0.6 times the pipe radius [32]. Later, this phenomenon has been adapted to microfluidics and has been studied for non-circular channel geometries. In the simplest case, for a straight channel with a square cross section, it was shown that after traveling a few cm from the inlet, particles migrate to four stable equilibrium positions in the vicinity of the channel wall centers [23,27]. For rectangle cross section, these equilibrium points collapse to two points near the center of the long walls [28,33]. Inertial focusing in channels with different cross sections including triangle and semi-circle was also investigated. It was shown that by combining these geometries in a specific sequence, it is possible to focus particles in a single train [29]. In all these geometries, the balance between inertial lift forces determines the equilibrium positions. However, for the separation of particles with different sizes, inertial effects may not suffice since equilibrium positions can be very close to each other. Thus, secondary flows in lateral direction are introduced to separate different size of particles with higher resolution.

To generate secondary flow, curved and microstructured channels (expansion-extraction, micro-pillars, and arc-shaped grooves) have been introduced. Expansion-extraction geometry has been studied extensively. It has been shown that this geometry is capable of separating particles and cells of different sizes [34]. Amini et al. demonstrated the effect of position and number of the pillars on secondary flow transformation and their effect on particle motion [35]. Later, Stoecklein et al. developed a framework to predict inertial flow transformations [36]. Straight channel with arc-shaped groove arrays is another structure capable of 3D focusing of particles [37]. Curvedchannels in different formats, including spiral [19,24,38,39] and serpentine [23,26,40,41], have been investigated both experimentally and numerically. Curved channel shape introduces two transverse vortices as secondary flow. The secondary flow is characterized by Dean number which is defined as $De = Re\sqrt{\frac{D_h}{2R}}$ where Re, D_h, and R are Reynolds number, hydraulic diameter, and radius of curvature respectively. To have a constant Dean number along a channel with constant hydraulic diameter and flow rate, radius of curvature should be kept constant. A ring shaped microchannel yields constant Dean number, though it is not practical to implement experimentally. Another option is to fabricate a 3D helical channel with constant radius. However, it is challenging to fabricate 3D structures using conventional microfabrication techniques, especially when at least one dimension of the channel is very small (<50 μm).

There are few studies that have investigated 3D channel structures. Paie et al. fabricated all-glass 3D microchannel with straight and curving loops achieving single spot particle focusing using femtosecond laser micromachining [42]. Lee et al. fabricated a helical microchannel using stereolithography based 3D-printer to detect pathogenic bacteria [43]. Xi et al. introduced the extrusion and curing of PDMS to construct elastomeric microtubes and investigated particle focusing efficiency inside circular microtubes with helical geometry [44]. Recently, Jung et al. used PDMS-parylene thin-film microfluidic system for shaping 3D channels and studied inertial focusing in helical microchannel. Although this technique allows to form flexible 3D structures, it requires multiple steps for preparation of PDMS-parylene device increasing the complexity of fabrication [45].

In this work we present a fabrication technique to study migration of particles in 2D and 3D layouts. The strength of the presented microfabrication technique comes from the fact that it relies on standard soft lithography methods while offering several unique 3D microfabricated structures that are far more challenging to achieve using alternative techniques. We introduce a novel double spiral channel configuration for 3D focusing. As discussed hitherto, due to the symmetric vortices, particles tend to focus in two streams in planar structures. To overcome this constraint, two spiral channels perpendicular to each other should be coupled to obtain single line focusing. Here, by leveraging our 3D fabrication technique, we were able to achieve a double oriented spiral (snail-like) channel geometry and studied inertial migration of particles.

2. Materials and methods

PDMS soft lithography is a common method used for the fabrication of microfluidic structures [46,47]. Here, we used soft lithography to have simple microchannel that are later morphed into 3D shapes. For mold fabrication, SU-8 2050 photoresist (Microchem Corp.) was patterned on silicon substrate. A channel height of 50 μm was obtained by spinning the photoresist at 3000 rpm for 40 s, for the fabrication of 2D structures including straight, spiral, and squarel designs. UV exposure was completed with 180 mJ/cm^2 dose. After post baking (65 °C for 3 min, 95 °C for 10 min, and 65 °C for 2 min) followed by 7 min development, the mold fabrication was completed. The helical structure is originated from a straight channel of 80 mm length, 50 μm width and 200 μm height. 200 μm channel height was reached by spinning the photoresist at 1000 rpm for 40 s. UV exposure was completed with 250 mJ/cm^2 dose. After post baking (65 °C for 15 min, 95 °C for 45 min, and 65 °C for 10 min) and 17 min of development, the mold fabrication was completed. The remaining fabrication steps are schematically illustrated in Fig. 1. After preparing the mold, PDMS mixture was prepared by mixing the base polymer and cur-

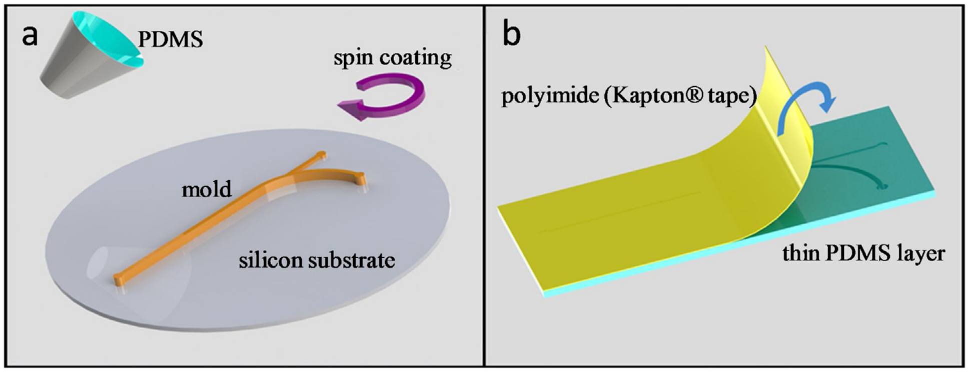

Fig. 1. Schematic of fabrication steps: a) PDMS is poured on the mold and spin-coated to a uniform thickness. b) The thin PDMS layer is peeled off and sealed with one side adhesive polyimide tape (Kapton®).

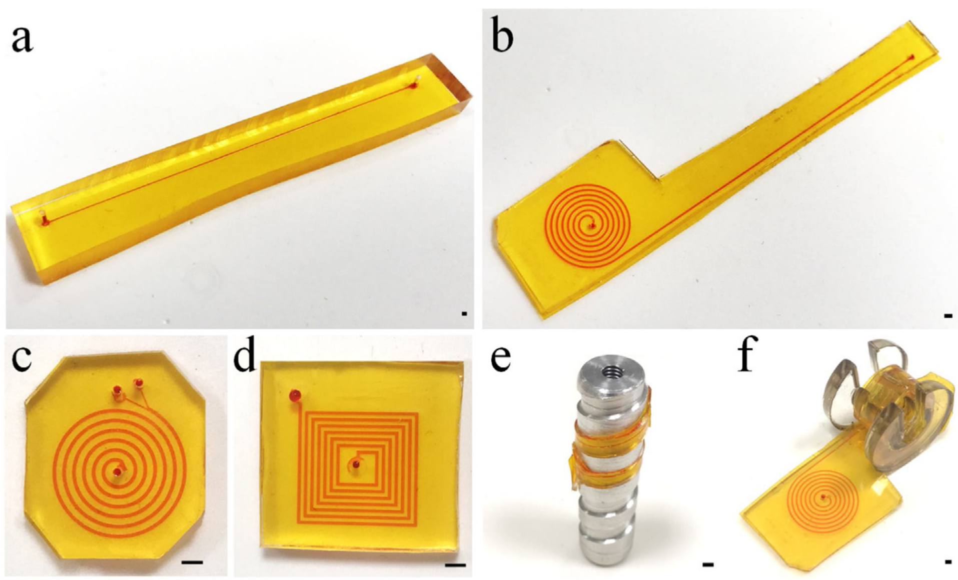

Fig. 2. Various 2D and 3D structures including straight (a), spiral (b, c), squarel (d), helical (e) and double oriented spiral (f) configured by using our simple technique. Scale bars are 1 mm.

ing agent at a ratio of 5:1 to achieve both flexibility of the structure and rigidity of the microchannel to maintain the cross-sectional shape. Then, the process was followed by degassing and pouring of the mixture onto the mold. To have a uniform PDMS layer, PDMS was spun on the mold using a two-step coating process to obtain 1 mm thick PDMS. For the channel dimensions showed in this study, 1 mm-thick PDMS provided the structural rigidity as well as the flexibility for the 3D shaping. The first layer was coated at 200 rpm for 60 s and cured on a hot plate at 90 °C for 5 min. Then, the second layer was coated at 100 rpm for 60 s and cured at 90 °C for 3 h. Then, PDMS is peeled off.

To finalize the fabrication of flexible devices, we seal the chips using 30 μm-thick Kapton® tape (Fig. 1b). This tape, when sealed to PDMS, can tolerate high pressures [48] and can be bent easily. Our bonding strength experiments revealed a burst pressure as high as 1200 mbar. This reversible, yet strong, sealing allows the user to delaminate the tape and replace it with a new tape, in case of any clogging in the channel. For repetitive sealing a slight decrease in bonding strength was observed experimentally at every iteration, as explained in detail in the supplementary document. Fig. 2 demonstrates the 2D (Fig. 2a–d) and 3D structures (2e and f) fabricated using this technique. To obtain the helical structures, aluminium posts with different diameters and pitches were prepared by CNC machining. Kapton taped PDMS layer was rolled along the grooves on the post (Fig. 2e, supplementary movie 1). For the snail-like structure, a polymethyl methacrylate (PMMA) holder has been fabricated by CO_2 laser machining (Epilog Zing 30 W) and the planar layout (Fig. 2b) was rolled on this holder to configure a double-oriented spiral (Fig. 2f). 6 μm diameter fluorescent YO Carboxylate microspheres are acquired from Polysciences Inc. (excitation/emission: 529/546 nm) to observe particle focusing within the fabricated structures by using florescence microscopy.

3. Results

In the first part of this study, inertial focusing in planar layouts has been investigated to examine the capability of the introduced fabrication method for inertial microfluidic systems. Moreover, an additional planar layout called squarel structure is introduced. For straight channel (width: 50 μm, height: 200 μm), 6 μm diameter particles are introduced from the inlet with different flow rates. Flow rates of 1, 5, 10, 15, and 20 ml/h have been examined. As shown in Fig. 3a, by increasing the flow rate, particles tend to align in two stream lines while traveling along the channels. The dominant force to align particles in two streams for straight microchannel is the inertial lift force. Next, the particles are introduced to the spiral microchannel (width: 300 μm height: 50 μm). Due to the curvature of the spiral channel structure, two vortices are created inside the

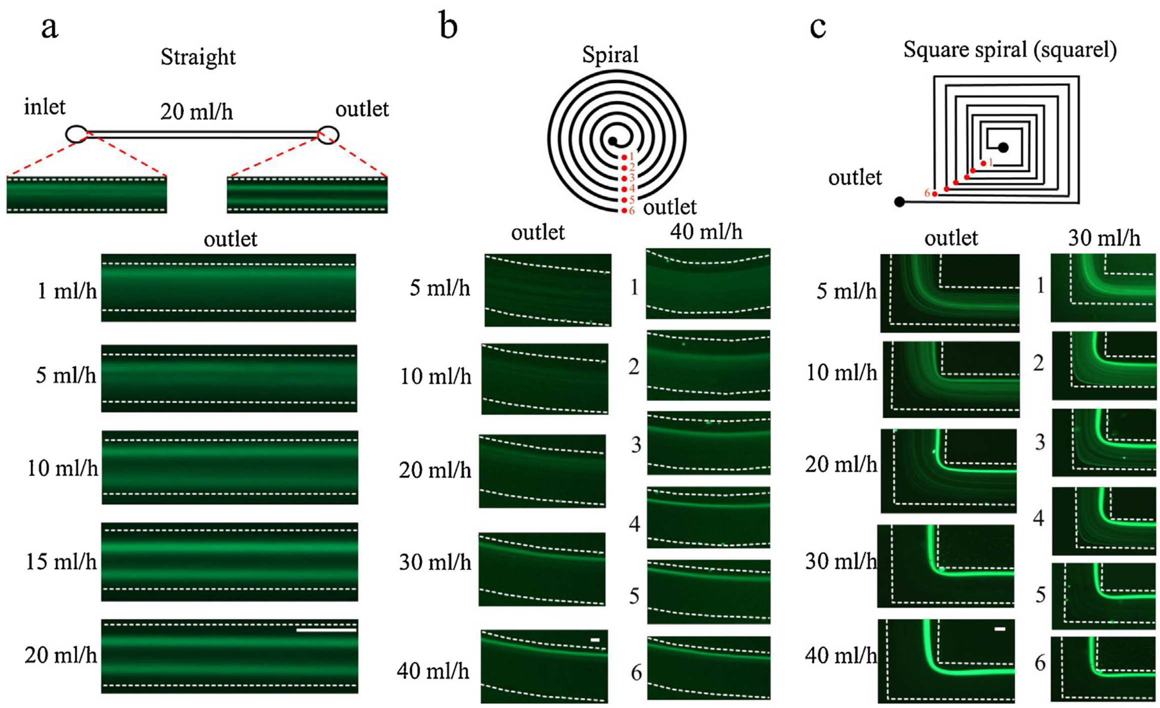

Fig. 3. Inertial focusing of particles in 2D structures. a) In straight channel particles align in two regions. b) In spiral channel particles align to a narrow region near inner wall by increasing the flow rate c) In squarel channel increasing the flow focuses the particles in a region near the inner wall. Scale bars are 50 μm.

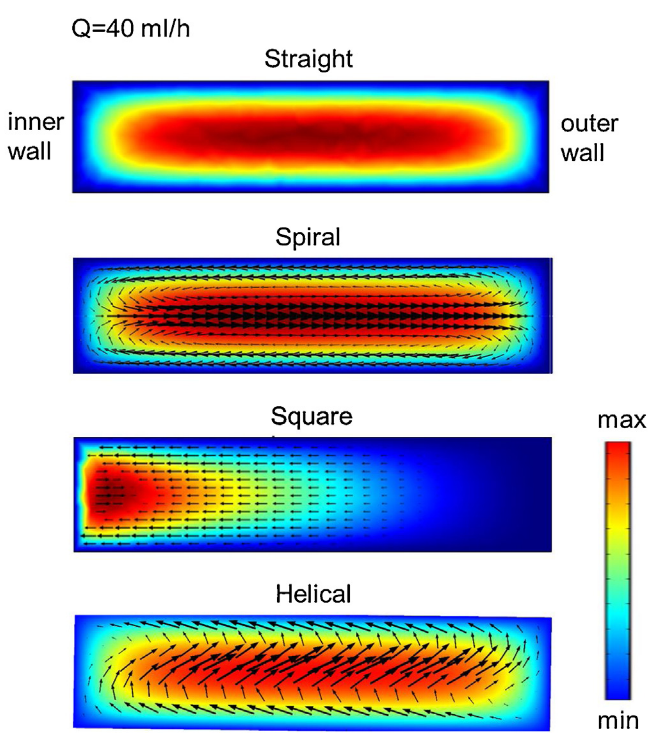

Fig. 4. Channel cross-sectional view of finite element analysis results of secondary flow in straight, spiral, squarel, and helical microchannels. Flow rate of 40 ml/h was chosen for all the cases, channel width is 200 μm, height is 50 μm. The color plot denotes relative velocity field, arrows denote secondary flow direction.

fluid (Fig. 4). These vortices generate a Dean drag force that affect particle lateral motion.

For the spiral design, Dean drag and inertial lift forces are introduced to the particles. As shown in Fig. 3b, flow rates of 5, 10, 20, 30, and 40 ml/h have been tested. By increasing the flow rate, inertial lift force further pushes the particles to the center of the microchannel, while particles are propelled to a region near the inner wall by the Dean drag force. At steady-state, particles equilibrate near the inner wall. Then, squarel design (width: 300 μm height: 50 μm) was tested for focusing of 6 μm diameter particles. Here, similar to the spiral design, the effective forces are inertial and Dean drag forces. However, there is a subtle but critical difference compared to spiral design. For spiral design, due to the continuous curvature, Dean drag force together with inertial force are continuously exerted on the particles. Contrarily, for the squarel design Dean force is exerted only at the sharp corners (Fig. 4). Therefore, for squarel design, particles first align to the center due to the inertial lift force. When the particles reach the corners, the dominant Dean force pushes them toward the inner wall. Finally, the particles rest near the inner wall. For this structure, flow rates of 5, 10, 20, 30, and 40 ml/h have been examined. As shown in Fig. 3c, increasing the flow rate squeezes the particles into a narrower region near the inner wall.

To study the effect of geometry on secondary flow formation, finite element analysis was done using Comsol v5.4. Straight, spiral, squarel, and helical channels were created with the same cross section (width: 200 μm height: 50 μm). The laminar flow with continuity and momentum balance was applied. For the inlet and outlet, constant flow rate of 40 ml/h and atmospheric pressure were set, respectively. In Fig. 4, the color plot denotes velocity distrubution; arrow field shows secondary flow direction.

For 3D structures, a helical microchannel has been configured from a straight channel using two templates with different pitches (4 and 8 mm) and focusing performance has been evaluated. The main difference between the helical and planar spiral configuration is that Dean vortices are not symmetric and the helix pitch distorts the vortices (Fig. 4). We have studied the pitch distortion effect on the migration of particles in helical structure by changing the helix pitch and the flow rate. The fabrication steps of the 3D helical channels are explained in detail in the Materials and Methods section and are also briefly shown in the supplementary movie 1. We would like to emphasize that the “tape’n roll” method allows easy modification of the helix pitch. We have prepared two alu-

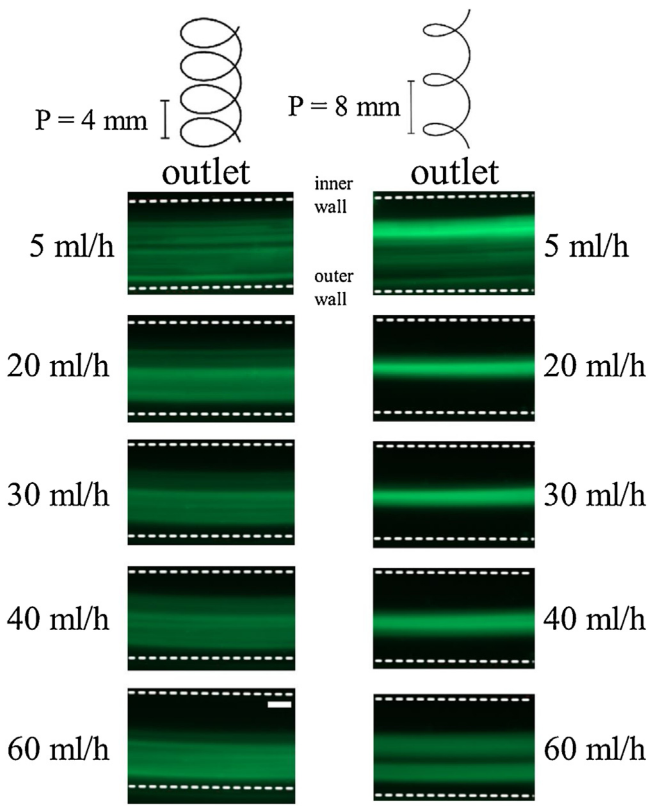

Fig. 5. Inertial migration in helical structure. For P = 4 mm, particles cover the half of the microchannel by increasing the flow rate. For P =8 mm and low flow rates, particles focus in the center and increasing the flow rate, resutls in revealing the both focusing regions. Scale bar is 50 µm for each figure.

minum rods with 6 mm diameter with pitch (P) of 4 and 8 mm. We used the same mold to obtain two 8 cm-long PDMS microchannels with an aspect ratio of 4 (w = 50 µm, h = 200 µm). These channels are sealed by Kapton® tape and rolled over the rods to obtain the helical channels with different pitches.

Experimental observations of the helical structure were done using side view imaging. We have varied the flow rate as 5, 20, 30, 40, and 60 ml/h for two different pitches 4 and 8 mm. The microscopy images for all test conditions are given in Fig. 5. Background image subtraction was performed for clarity of the focusing performance. Increasing the flow rate results in the squeezing of the particles near the wall when the pitch is equal to 4 mm. When we used 8 mm pitch, particles are wide spread in the microchannel at low flow rate (5 ml/h). Increasing the flow rate results in the formation of focusing of the particles at the center of the channel in the 20–40 ml/h flow rate range. By further increase of the flow rate to 60 ml/h, particles tend to align at two focusing regions. This effect shows the importance of the geometrical parameters and the flow conditions on particle focusing behavior. Beside, by using the 3D helical channels, double train focusing displacement can be observed by simply changing the helix pitch.

Particle focusing can be studied in detail if the particles can be tracked in a given flow field. Experimental approaches for particle tracking are cumbersome and require registering the particles and capturing their cross-sectional position at several locations along the channel. As an alternative, computational modeling provides the trajectories for particles and allows thorough analysis of focusing performance. However, since the ratio of channel length to hydraulic diameter is high, it requires considerable computational cost to track finite size particles. Here, we propose an alternative method to investigate particle migration inside the microchannel that is not restricted for the geometries introduced in this article and can be applied more generally. First, the geometry is sketched in a 3D CAD software (Solidworks) and imported to a finite element modeling software (Comsol) to solve the flow field in the channel in the absence of suspended particles. Then, the flow velocities from Comsol are fed to a Matlab algorithm, using Comsol-Matlab link, and the position of the particles were traced iteratively to obtain particle trajectory as schematically shown in Fig. 6. For simplicity, particles are taken as point objects; particle-particle interactions and flow field disturbances due to particle motion are neglected. The Lagrangian discrete phase model was used to determine particle trajectory based on the geometry of the channel and exerted forces. By using Newton's second law, force balance equation for a single particle can be writtenas:

$$\sum F = m_p a_p \tag{1}$$

Where $\boldsymbol{m_p}$, $\boldsymbol{a_p}$, and F are particle mass, acceleration, and the forces acting on the particle. For a particle moving inside Newtonian fluid at inertial regime, the effective forces are: inertial lift force ($\boldsymbol{F_L}$), drag force ($\boldsymbol{F_D} = 6\pi\boldsymbol{\mu R_p}(\boldsymbol{u_f} - \boldsymbol{u_p})$), buoyancy ($\boldsymbol{F_B} = (\boldsymbol{\rho_p} - \boldsymbol{\rho_f})\boldsymbol{V_p g}$), and virtual mass force due to acceleration difference between particle and fluid ($\boldsymbol{F_v} = \frac{1}{2}\boldsymbol{\rho_f V_p}(\boldsymbol{a_f} - \boldsymbol{a_p})$). Here, Stokes drag force is considered since particle lateral velocity is low enough resulting in small Reynolds number in lateral direction and particle initial velocity is considered the same as the fluid velocity to neglect the particle slip. For lift force, several analytical expressions have been developed [49–51]. Hood et al. derived inertial force function for rectangular channels with different aspect ratios by using asymptotic theory. It was verified experimentally by using sub-pixel accurate particle tracking and velocimetric reconstruction of the depth dimension for rectangular channel with aspect ratio (AR) of two [52]. Here, Hood's lift force is implemented for AR of 1, 2, 4 and 8 [49,52–54]. By simplifying all the effective forces in Eq. (1), we can reach to:

$$a_p = \frac{2}{(2\rho_p + \rho_f)V_p}\Big[F_L + 6\pi\mu R_p\left(u_f - u_p\right) + \left(\rho_p - \rho_f\right)V_p g + \frac{1}{2}\rho_f V_p a_f\Big] \tag{2}$$

Recently, Rasooli et al. introduced computational modeling approach by using Crank-Nicolson temporal integrator to study inertial migration of particles in spiral microchannels. [39] Here, we implement the fourth order Runga-Kutta technique to solve the differential equation. The particle tracking algorithm is explained in detail in the supplementary file. The computational particle migration results are analyzed as summarized in Fig. 6. The particles are uniformly distributed at the inlet. As they move along the channel, they get focused and they reach to a steady-state focused profile, given enough distance. The focused particle trajectory is an elliptical shape across the channel cross section. Based on the geometry, flow condition, and particle size; the location (d_x, d_z) and the size of the ellipse (R_x, R_z) change (Fig. 6c), which is analyzed in detail using the computational method.

Helix pitch is a parameter that affects particle equilibrium state and position, which is unique to our 3D channel geometry. For planar layout where there is no pitch, the Dean flow is symmetric. For the upper and lower half of the microchannel near the zero lift force lines, the fluid flow is toward the inner wall. Based on the balance between the lift force and the Dean force, the equilibrium position changes. However, having a 3D helical channel, *i.e.* by adding pitch to the structure, the Dean flows become asymmetric. For smaller pitches, this asymmetry effect is not significant to affect the particle motion. However, after sufficiently high pitch value, in the upper half of the microchannel near the zero lift force line, the Dean flow

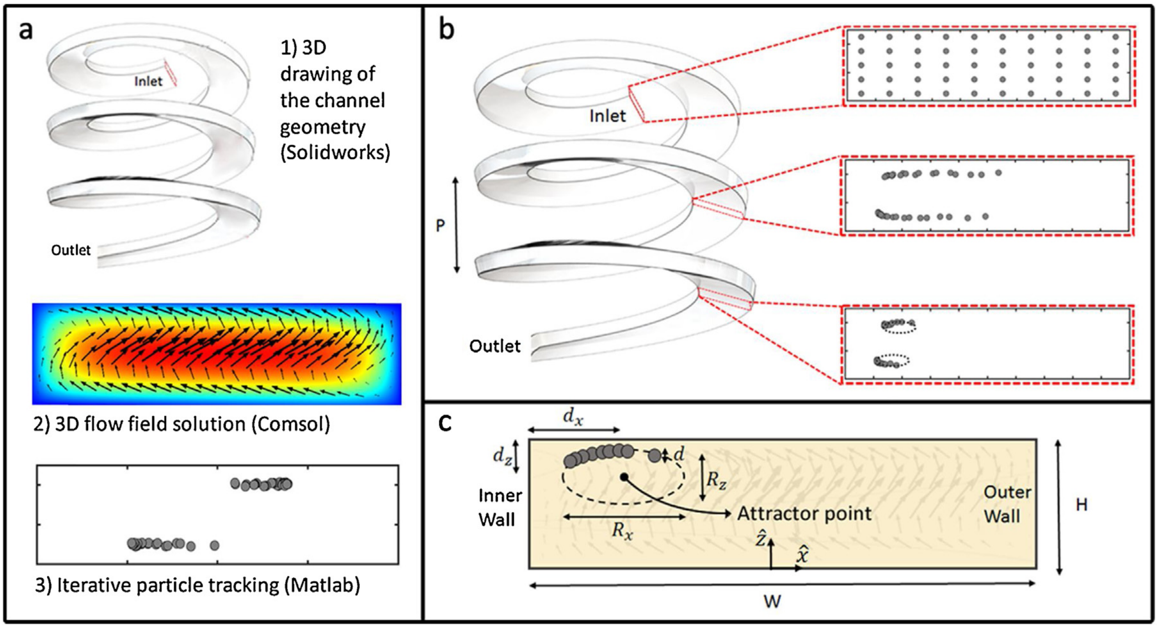

Fig. 6. The computational approach used to study inertial migration of particles inside helical channels. a) First, the geometry is sketched using a 3D CAD software. Afterwards, using the boundary conditions, flow field is solved by a finite element analysis software. Finally, the position of particles along the channel is determined by Lagrangian discrete phase model. b) Uniformly distributed particles are released from the inlet. First, they are focused in two pre-focusing lines due to dominance of inertial forces. Then, they occupy two ellipse shape regions due to the competition of inertial and Dean forces. c) Geometrical parameters of inertial migration for helical channel: d_x, d_z, R_x, R_z, H, and W correspond to ellipse center distance from inner wall, distance from upper wall, ellipse diameter in x direction, ellipse diameter in z direction, height, and width of the channel. The arrows in the background illustrate Dean flow field.

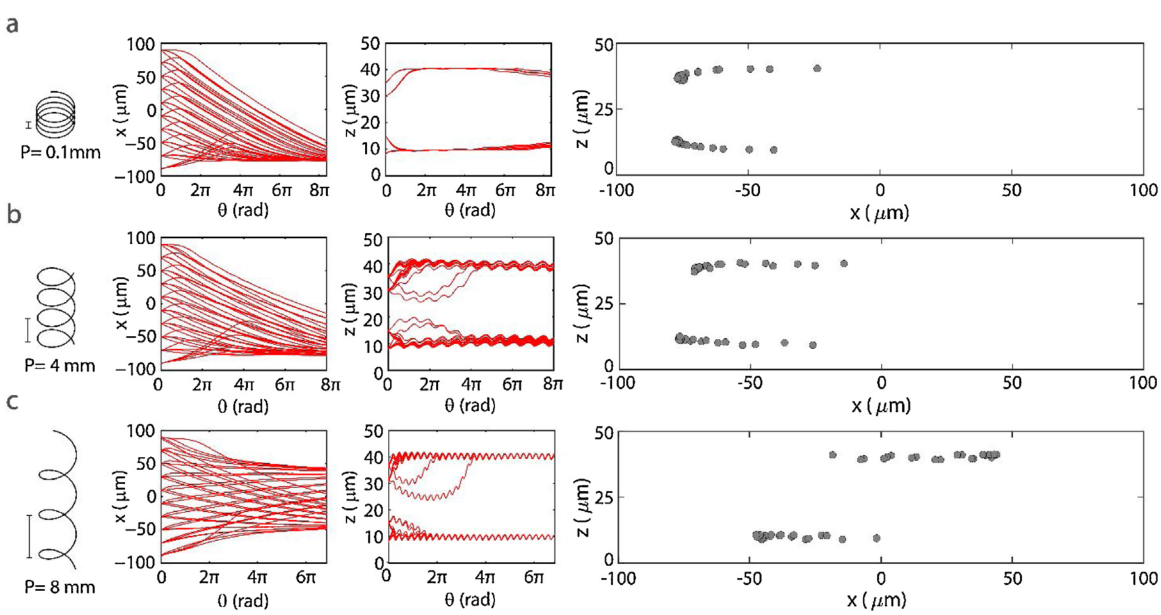

Fig. 7. Trajectory of the microparticles obtained for varying helix pitch using the computational approach. The flow rate (Q = 60 ml/h), helix diameter (D = 6 mm), particle diameter (d = 6 μm), and aspect ratio (AR = 4) are kept constant. Helix pitch is changed as a) 0.1 mm b) 4 mm and c) 8 mm.

points toward the outer wall resulting in particle focusing far from the inner wall. Fig. 7 shows the particle trajectory and final status of focusing for different pitch values. As can be observed from Fig. 7a, for 0.1 mm pitch, 6 μm diameter particles are focused near the inner wall. The two attractor points (for the upper and lower half of the channel) are almost at the same x position. For 4 mm pitch length (Fig. 7b), there is small misalignment of the particle focusing points. Increasing the pitch to 8 mm (Fig. 7c) results in the migration of the upper attractor point near the outer wall. Additionally, particles have an oscillatory trajectory in vertical direction for both 4 mm and 8 mm pitches.

For the case of 8 mm pitch and for a particle in the upper left quarter of the channel, the lift force and Dean drag force are both in the same direction and point toward the outer wall. After reaching the upper right quarter of the channel, the lift force changes direction toward the inner wall opposing the Dean force. This com-

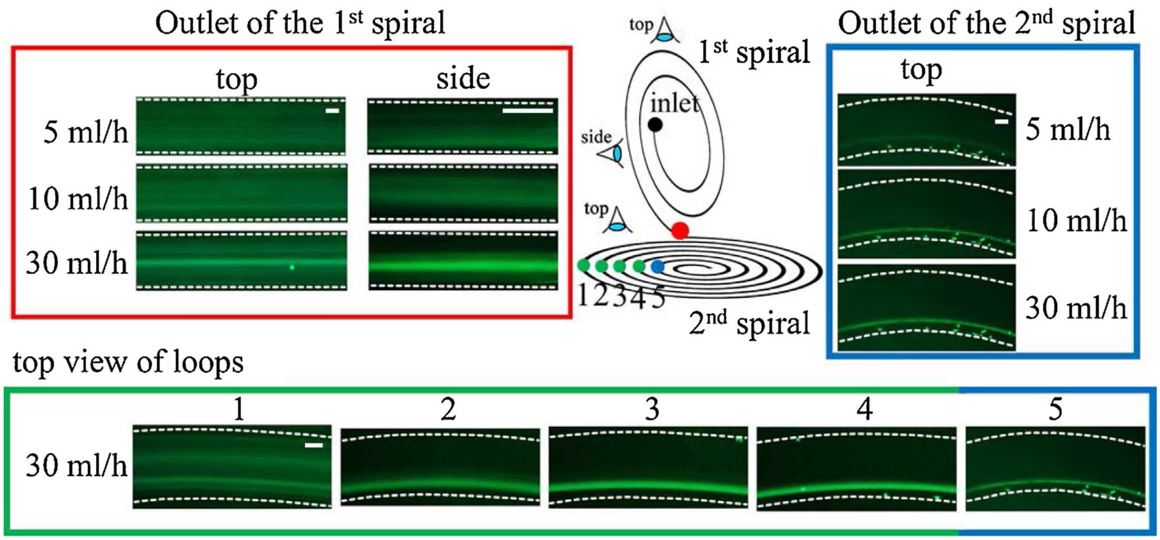

Fig. 8. Particle focusing in double oriented spiral geometry. For the first spiral, particles are aligned in one direction. Second spiral aligns the particles in a single file. Scale bars are 50 μm.

petition causes the particles to focus in a point near the outer wall. However, for the particles in the lower half of the channel similar to planar structures, the Dean flow points toward the inner wall, which assists the particle to settle at a point near the inner wall.

We have also studied the effect of helix diameter (supplementary movie 2), particle size (supplementary movie 3), flow rate and aspect ratio on particle focusing trajectory as given in the supplementary document. These results demonstrate the strength of the computational approach that provide the means to study the influence of all effective parameters in detail. Application of this method to 3D geometries would lead to a much faster design optimization cycle compared to experimental approaches.

Finally, the flexibility of the tape'n rolled structure was exploited to configure a snail-like structure as shown in Fig. 2f. This structure is used to obtain single stream inertial focusing. As shown in Fig. 8, particles are introduced from the vertical spiral and collected from the planar spiral. For the first spiral, increasing the flow rate results in squeezing of particles in a region when looking from side. However, for the top view particles are not squeezed in a single profile. To achieve focusing into a single line, which is very critical for all particle characterization applications, the second spiral is used. This second channel segment produces Dean vortices perpendicular to the previous spiral. Therefore, it helps to focus the particles in both directions. By increasing the flow rate from 5 to 30 ml/h, single line focusing can be achieved. This result shows how single line focusing in inertial microfluidics can be achieved by using such a simple fabrication technique.

Some of the key points obtained from these results are summarized below:

1 For 3D helical design, the radius of curvature is kept constant, however, helix pitch distorts the symmetry of the Dean vortices. Increasing the helix pitch skews the position of the two attractor points. Therefore, to avoid diagonal focusing of the particles, helix pitch should be as small as possible.
2 Tape'n rolled designs allow to configure planar layouts in an orthogonal structure and obtain single line focusing of particles.
3 The tape'n roll fabrication method allows facile modification of the channel structure while maintaining the channel cross section and the length. Additionally, in case of any clogging or contamination, the tape can be removed and the structures can be cleaned and reconstructed in minutes.

4. Conclusions

Fabrication of 3D microfluidic device is still a challenging task. Here, we report novel 2D and 3D microstructures enabled by a low-cost and rapid fabrication technique. Kapton® tape as an easily accessible material gives the required flexibility together with strong sealing for PDMS microchannels. From a plethora of applications for such a fabrication method, we exploited inertial microfluidics. First, inertial focusing using planar layouts was shown and a novel squarel geometry was introduced. This new channel design has much easier machineability as it consists of straight lines. Most design transfering systems work in cartesian coordinates with two actuators in each axis, hence can achieve precision manufacturing of vertical and horizontal geometries. However, spiral geometry as one of the most commonly used inertial microfluidics design, is much more demanding on the manufacturing instrument. Hence, squarel geometry offers fabrication of inertial microfluidics devices with increased precision owing to its straight geometry. Tape'n roll technique enables easy fabrication of 3D microchannels by rolling standard 2D planar microchannels. Kapton® tape has manifested good sealing ensuring flexibility in 3D micro channels as well. Helical microchannels were fabricated by simply winding a straight microchannel around a cylindrical post. The effect of flow rate and helical pitch were investigated experimtentally by monitoring migration of fluorescent beads under optical microscope. We have also developed a computational method to gain a thorough understanding of particle motion in helical channels and also to assist in the design optimization process. In helical structures, although the radius of curvature is constant, particles cannot be confined in a single line due to the distortion of Dean vortices resulting from the helix pitch. The double oriented spiral design overcomes this issue. The first spiral is configured by rolling a straight microchannel around a holder perpendicular to the planar spiral. The first spiral focuses the particles to a single plane where the second spiral confines the particles to a single line achieving an ideal focusing. As a practical and inexpensive method, tape'n roll fabrication can lead to many more intricate geometries and pave the way for interesting microfluidic applications. We spot wearable sensors as one of the potential areas to explore.

Acknowledgements

The authors thank Reza Rasooli, Pinar Beyazkilic, and Ziya Isiksacan for helpful discussion and critical reading of the manuscript. Special thanks goes to Dr. Kaitlyn Hood for providing the inertial lift force codes for rectangular channel cross sections of different aspect ratios.

Appendix A. Supplementary data

Supplementary material related to this article can be found, in the online version, at doi:https://doi.org/10.1016/j.sna.2019.111630.

References

[1] A.A.S. Bhagat, H. Bow, H.W. Hou, S.J. Tan, J. Han, C.T. Lim, Microfluidics for cell separation, Med. Biol. Eng. Comput. 48 (2010) 999–1014.
[2] D.R. Gossett, W.M. Weaver, A.J. Mach, S.C. Hur, H.T.K. Tse, W. Lee, et al., Label-free cell separation and sorting in microfluidic systems, Anal. Bioanal. Chem. 397 (2010) 3249–3267.
[3] M.E. Warkiani, A.K.P. Tay, B.L. Khoo, X. Xiaofeng, J. Han, C.T. Lim, Malaria detection using inertial microfluidics, Lab Chip 15 (2015) 1101–1109.
[4] D. Holmes, H. Morgan, N.G. Green, High throughput particle analysis: combining dielectrophoretic particle focussing with confocal optical detection, Biosens. Bioelectron. 21 (2006) 1621–1630.
[5] Y. Zhao, B.S. Fujimoto, G.D. Jeffries, P.G. Schiro, D.T. Chiu, Optical gradient flow focusing, Opt. Express 15 (2007) 6167–6176.
[6] L. Liang, X. Xuan, Diamagnetic particle focusing using ferromicrofluidics with a single magnet, Microfluid. Nanofluidics 13 (2012) 637–643.
[7] J. Shi, S. Yazdi, S.-C.S. Lin, X. Ding, I.-K. Chiang, K. Sharp, et al., Three-dimensional continuous particle focusing in a microfluidic channel via standing surface acoustic waves (SSAW), Lab Chip 11 (2011) 2319–2324.
[8] H. Amini, W. Lee, D. Di Carlo, Inertial microfluidic physics, Lab Chip 14 (2014) 2739–2761.
[9] K.W. Seo, H.J. Byeon, H.K. Huh, S.J. Lee, Particle migration and single-line particle focusing in microscale pipe flow of viscoelastic fluids, RSC Adv. 4 (2014) 3512–3520.
[10] M. Asghari, M. Serhatlioglu, B. Ortaç, M.E. Solmaz, C. Elbuken, Sheathless microflow cytometry using viscoelastic fluids, Sci. Rep. 7 (2017) 12342.
[11] M. Serhatlioglu, M. Asghari, M. Tahsin Guler, C. Elbuken, Impedance-based viscoelastic flow cytometry, Electrophoresis 40 (2019) 906–913.
[12] S.C. Hur, H.T.K. Tse, D. Di Carlo, Sheathless inertial cell ordering for extreme throughput flow cytometry, Lab Chip 10 (2010) 274–280.
[13] X. Wang, H. Gao, N. Dindic, N. Kaval, I. Papautsky, A low-cost, plug-and-play inertial microfluidic helical capillary device for high-throughput flow cytometry, Biomicrofluidics 11 (2017), 014107.
[14] S. Kahkeshani, H. Haddadi, D. Di Carlo, Preferred interparticle spacings in trains of particles in inertial microchannel flows, J. Fluid Mech. 786 (2016).
[15] J.F. Edd, D. Di Carlo, K.J. Humphry, S. Köster, D. Irimia, D.A. Weitz, et al., Controlled encapsulation of single-cells into monodisperse picolitre drops, Lab Chip 8 (2008) 1262–1264.
[16] R. Khojah, R. Stoutamore, D. Di Carlo, Size-tunable microvortex capture of rare cells, Lab Chip 17 (2017) 2542–2549.
[17] H. Haddadi, D. Di Carlo, Inertial flow of a dilute suspension over cavities in a microchannel, J. Fluid Mech. 811 (2017) 436–467.
[18] W.C. Lee, A.A.S. Bhagat, S. Huang, K.J. Van Vliet, J. Han, C.T. Lim, High-throughput cell cycle synchronization using inertial forces in spiral microchannels, Lab Chip 11 (2011) 1359–1367.
[19] G. Guan, L. Wu, A.A. Bhagat, Z. Li, P.C. Chen, S. Chao, et al., Spiral microchannel with rectangular and trapezoidal cross-sections for size based particle separation, Sci. Rep. 3 (2013) 1475.
[20] M.E. Warkiani, B.L. Khoo, L. Wu, A.K.P. Tay, A.A.S. Bhagat, J. Han, et al., Ultra-fast, label-free isolation of circulating tumor cells from blood using spiral microfluidics, Nat. Protoc. 11 (2016) 134.
[21] S.C. Hur, S.-E. Choi, S. Kwon, D.D. Carlo, Inertial focusing of non-spherical microparticles, Appl. Phys. Lett. 99 (2011), 044101.
[22] M. Masaeli, E. Sollier, H. Amini, W. Mao, K. Camacho, N. Doshi, et al., Continuous inertial focusing and separation of particles by shape, Phys. Rev. X 2 (2012), 031017.
[23] D. Di Carlo, D. Irimia, R.G. Tompkins, M. Toner, Continuous inertial focusing, ordering, and separation of particles in microchannels, Proc. Natl. Acad. Sci. 104 (2007) 18892–18897.
[24] S.S. Kuntaegowdanahalli, A.A.S. Bhagat, G. Kumar, I. Papautsky, Inertial microfluidics for continuous particle separation in spiral microchannels, Lab Chip 9 (2009) 2973–2980.
[25] A. Russom, A.K. Gupta, S. Nagrath, D. Di Carlo, J.F. Edd, M. Toner, Differential inertial focusing of particles in curved low-aspect-ratio microchannels, New J. Phys. 11 (2009), 075025.
[26] J. Zhang, S. Yan, R. Sluyter, W. Li, G. Alici, N.-T. Nguyen, Inertial particle separation by differential equilibrium positions in a symmetrical serpentine micro-channel, Sci. Rep. 4 (2014) 4527.
[27] Y.-S. Choi, K.-W. Seo, S.-J. Lee, Lateral and cross-lateral focusing of spherical particles in a square microchannel, Lab Chip 11 (2011) 460–465.
[28] J. Zhou, I. Papautsky, Fundamentals of inertial focusing in microchannels, Lab Chip 13 (2013) 1121–1132.
[29] J.-A. Kim, J. Lee, C. Wu, S. Nam, D. Di Carlo, W. Lee, Inertial focusing in non-rectangular cross-section microchannels and manipulation of accessible focusing positions, Lab Chip 16 (2016) 992–1001.
[30] J.S. Choi, Y. Piao, T.S. Seo, Fabrication of a circular PDMS microchannel for constructing a three-dimensional endothelial cell layer, Bioprocess Biosyst. Eng. 36 (2013) 1871–1878.
[31] J.C. Yeo, C.T. Lim, Emerging flexible and wearable physical sensing platforms for healthcare and biomedical applications, Microsyst. Nanoeng. 2 (2016) 16043.
[32] G. Segre, A. Silberberg, Radial particle displacements in Poiseuille flow of suspensions, Nature 189 (1961) 209.
[33] D. Di Carlo, J.F. Edd, K.J. Humphry, H.A. Stone, M. Toner, Particle segregation and dynamics in confined flows, Phys. Rev. Lett. 102 (2009), 094503.
[34] Z. Wu, Y. Chen, M. Wang, A.J. Chung, Continuous inertial microparticle and blood cell separation in straight channels with local microstructures, Lab Chip 16 (2016) 532–542.
[35] H. Amini, E. Sollier, M. Masaeli, Y. Xie, B. Ganapathysubramanian, H.A. Stone, et al., Engineering fluid flow using sequenced microstructures, Nat. Commun. 4 (2013) 1826.
[36] D. Stoecklein, C.-Y. Wu, K. Owsley, Y. Xie, D. Di Carlo, B. Ganapathysubramanian, Micropillar sequence designs for fundamental inertial flow transformations, Lab Chip 14 (2014) 4197–4204.
[37] Q. Zhao, J. Zhang, S. Yan, D. Yuan, H. Du, G. Alici, et al., High-throughput sheathless and three-dimensional microparticle focusing using a microchannel with arc-shaped groove arrays, Sci. Rep. 7 (2017) 41153.
[38] J.M. Martel, M. Toner, Particle focusing in curved microfluidic channels, Sci. Rep. 3 (2013) 3340.
[39] R. Rasooli, B. Çetin, Assessment of lagrangian modeling of particle motion in a spiral microchannel for inertial microfluidics, Micromachines. 9 (2018) 433.
[40] D. Jiang, W. Tang, N. Xiang, Z. Ni, Numerical simulation of particle focusing in a symmetrical serpentine microchannel, RSC Adv. 6 (2016) 57647–57657.
[41] J. Zhang, D. Yuan, Q. Zhao, A.J.T. Teo, S. Yan, C.H. Ooi, W. Li, N.-T. Nguyen, Fundamentals of differential particle inertial focusing in symmetric sinusoidal microchannels, Anal. Chem. 91 (2019) 4077–4084.
[42] P. Paiè, F. Bragheri, D. Di Carlo, R. Osellame, Particle focusing by 3D inertial microfluidics, Microsyst. Nanoeng. 3 (2017) 17027.
[43] W. Lee, D. Kwon, W. Choi, G.Y. Jung, A.K. Au, A. Folch, et al., 3D-printed microfluidic device for the detection of pathogenic bacteria using size-based separation in helical channel with trapezoid cross-section, Sci. Rep. 5 (2015) 7717.
[44] W. Xi, F. Kong, J.C. Yeo, L. Yu, S. Sonam, M. Dao, et al., Soft tubular microfluidics for 2D and 3D applications, Proc. Natl. Acad. Sci. 114 (2017) 10590–10595.
[45] B.-J. Jung, J. Kim, J.-a. Kim, H. Jang, S. Seo, W. Lee, PDMS-parylene hybrid, flexible microfluidics for real-time modulation of 3D helical inertial microfluidics, Micromachines 9 (2018) 255.
[46] D.C. Duffy, J.C. McDonald, O.J. Schueller, G.M. Whitesides, Rapid prototyping of microfluidic systems in poly (dimethylsiloxane), Anal. Chem. 70 (1998) 4974–4984.
[47] Z. Isiksacan, M.T. Guler, B. Aydogdu, I. Bilican, C. Elbuken, Rapid fabrication of microfluidic PDMS devices from reusable PDMS molds using laser ablation, J. Micromechanics Microengineering 26 (2016), 035008.
[48] M.V. Hoang, H.-J. Chung, A.L. Elias, Irreversible bonding of polyimide and polydimethylsiloxane (PDMS) based on a thiol-epoxy click reaction, J. Micromechanics Microengineering 26 (2016), 105019.
[49] K. Hood, S. Lee, M. Roper, Inertial migration of a rigid sphere in three-dimensional Poiseuille flow, J. Fluid Mech. 765 (2015) 452–479.
[50] C. Liu, C. Xue, J. Sun, G. Hu, A generalized formula for inertial lift on a sphere in microchannels, Lab Chip 16 (2016) 884–892.
[51] S. Asmolov, Evgeny, the inertial lift on a spherical particle in a plane Poiseuille flow at large channel Reynolds number, J. Fluid Mech. 381 (1999) 63–87.
[52] K. Hood, S. Kahkeshani, D. Di Carlo, M. Roper, Direct measurement of particle inertial migration in rectangular microchannels, Lab Chip 16 (2016) 2840–2850.
[53] K. Hood, First Release of Inertial Lift Force Rectangle AR4, 2017, http://dx.doi.org/10.5281/zenodo.833521, July 21 Accessed.
[54] K. Hood, First Release of Inertial Lift Force Rectangle AR8, 2017, http://dx.doi.org/10.5281/zenodo.833525, July 21, Accessed.

Biographies

Mohammad Asghari is now a Ph.D. candidate at ETH Zürich, Department of Chemistry and Applied Biosciences. He received his M.S. degree from UNAM, Materials Science and Nanotechnology program at Bilkent University. His research interests are in field of microfluidics, bioengineering, and point-of-care diagnostics.

Murat Serhatlioglu is a Ph.D. candidate at UNAM Materials Science and Nanotechnology Program at Bilkent University. He received his M.S. degree from Meliksah University. His research interests are in the field of microfluidics and optical integration, flow cytometry applications, single cell characterization, viscoelastic fluids and their microfluidic applications.

Resul Saritas is currently pursuing his Ph.D. at the Department of Systems Design Engineering, University of Waterloo. He received his master's degree from the Department of Mechanical Engineering, University of Waterloo, Canada. His research focuses on lab-on-a-chip platforms, triboelectric energy harvesting, field effect transistors (FET) and nanoscratching lithography.

Mustafa Tahsin Guler received his Ph.D. degree from Kirikkale University Department of Physics. After a post-doctoral study at Harvard Medical School, he is currently a visiting researcher at Bilkent University UNAM and research assistant at Kirikkale University. His research interest covers development of microfluidics components, rapid prototyping methods and micro-electrical biosensors.

Caglar Elbuken is an assistant professor at Bilkent University, National Nanotechnology Research Center. He obtained his B.Sc. degree in Electrical and Electronics Engineering at Bilkent University and his Ph.D. degree in Mechanical Engineering at University of Waterloo. His research interests include lab-on-a-chip devices, droplet microfluidics, point-of-care diagnostics, and viscoelastic fluids. He is the recipient of the Science Academy's 2019 Young Scientist Award.